JOURNAL OF SPACECRAFT AND ROCKETS
Vol. 46, No. 2, March–April 2009

Autonomous Aerobraking Using Thermal Response Surface Analysis

Jill L. Prince* and John A. Dec†
NASA Langley Research Center, Hampton, Virginia 23681
and
Robert H. Tolson‡
North Carolina State University, Hampton, Virginia 23666

DOI: 10.2514/1.32793

Aerobraking is a proven method of significantly increasing the science payload that can be placed into low Mars orbits when compared to an all propulsive capture. However, the aerobraking phase is long and has mission cost and risk implications. The main cost benefit is that aerobraking permits the use of a smaller and cheaper launch vehicle, but additional operational costs are incurred during the long aerobraking phase. Risk is increased due to the repeated thermal loading of spacecraft components and the multiple attitude and propulsive maneuvers required for successful aerobraking. Both the cost and risk burdens can be significantly reduced by automating the aerobraking operations phase. All of the previous Mars orbiter missions that have used aerobraking have increasingly relied on onboard calculations during aerobraking. Even though the temperature of spacecraft components has been the limiting factor, operational methods have relied on using a surrogate variable for mission control. This paper describes several methods, based directly on spacecraft component maximum temperature, for autonomously predicting the subsequent aerobraking orbits and prescribing apoapsis propulsive maneuvers to maintain the spacecraft within specified temperature limits. Specifically, this paper describes the use of thermal response surface analysis in predicting the temperature of the spacecraft components and the corresponding uncertainty in this temperature prediction.

Nomenclature

A	=	spacecraft area, m^2
A_n	=	amplitude of atmospheric wave n from atmospheric wave model
A_0	=	random variable accounting for unmodeled density variation
a_y	=	spacecraft acceleration in y direction, m/s^2
C_y	=	coefficient of drag; spacecraft y coordinate
h	=	altitude, km
h_s	=	atmospheric scale height, km
h_0	=	reference altitude, km
m	=	spacecraft mass, kg
P	=	orbital period, h
S	=	dust storm constant
V	=	spacecraft relative velocity, m/s
λ	=	east longitude, deg
λ_n	=	phase of atmospheric wave from atmospheric wave model
ρ	=	atmospheric density, kg/m^3
ρ_{nom}	=	baseline atmospheric density before inclusion of perturbation
ρ_0	=	atmospheric density at reference altitude
σ	=	standard deviation
φ	=	latitude, deg

Presented as Paper 861 at the 45th AIAA Aerospace Sciences Meeting and Exhibit, Reno, NV, 8–11 January 2007; received 13 June 2007; accepted for publication 7 March 2008.

*Aerospace Engineer, Exploration Systems Engineering Branch, Mail Stop 489. AIAA Member.
†Aerospace Engineer, Structural and Thermal Systems Branch, Mail Stop 431. AIAA Member.
‡Langley Professor, Mechanical and Aerospace Engineering Department 100 Exploration Way. AIAA Associate Fellow.

I. Introduction

AEROBRAKING is a proven method for increasing payload delivered to low Mars orbit. Typical mass saving is greater than the equivalent propulsive mass for a 1000 m/s Mars orbit insertion burn (approximately 450 kg for a 1700-kg spacecraft). After establishing a high-eccentricity, long period orbit, aerobraking reduces orbital period and eccentricity to a desired science orbit by passing through the upper atmosphere 300 or more times and using the drag on the spacecraft to reduce velocity. To achieve a successful aerobraking phase, enough drag must be accumulated such that the spacecraft reaches its final orbit in a relatively short amount of time, but there are limiting factors on the spacecraft that influence the rapidity of the aerobraking phase. The limiting factor for past aerobraking missions has been the maximum temperature limit of the spacecraft: temperatures must be kept low to avoid burning or melting of spacecraft components. Typically, the spacecraft component with the most limiting temperature qualification is the solar arrays, which are the main drag surfaces. Mars Reconnaissance Orbiter (MRO) had an additional limiting factor toward the end of aerobraking, which was the temperature of the onboard batteries. Aerobraking has been used successfully for the following NASA spacecraft currently orbiting Mars: Mars Global Surveyor (MGS) [1], Mars Odyssey [2], and MRO [3]. Because of orbit-to-orbit atmospheric density variation, the temperature of the solar arrays cannot be accurately predicted. At Mars, the average 1-σ orbit-to-orbit density variation [4] over the previous missions has been 40%. Depending on latitude and season, the orbit-to-orbit variability can range from 15 to 100%. Consequently, the aerobraking operations phase has required many teams (navigation, atmospheric scientist, mission designers, spacecraft, thermal analyst, etc.) to constantly monitor the mission throughout the aerobraking phase, which can last from 3 to 6 months. Automating this process reduces workload, cost, and risk of potential human error. Automation may also increase aerobraking mission flexibility in that maneuvers can be chosen that are outside of a predetermined menu of maneuvers that are loaded on the spacecraft periodically [5], rather than relying on ground-based personnel to choose a maneuver limited to optimal times within a common workday. In addition, all aerobraking

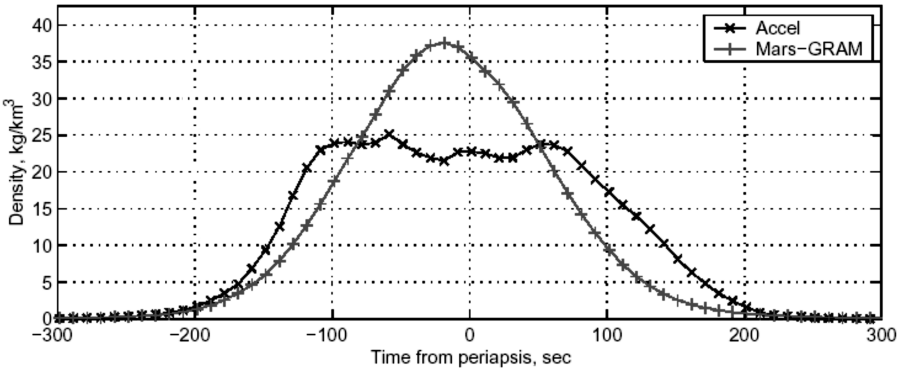

Fig. 1 Odyssey periapsis 157 density profile.

operations have used surrogate variables (maximum dynamic pressure or maximum freestream heat flux) for mission control in lieu of the real constraint: solar array temperatures.

After the Mars Global Surveyor aerobraking experience, which spanned 15 months and over 800 aerobraking passes, it became clear that building more autonomy into aerobraking could significantly reduce mission cost. Three methods of automating the aerobraking operations phase were subsequently developed with different levels of complexity to adjust the flight sequence based on density inferred by accelerometer measurements during the aerobraking pass [6,7]. The time to initiate the aerobraking sequence is important because the spacecraft must be oriented to aerobraking attitude before atmospheric entry and reorient to cruise attitude after exiting the atmosphere. Because of the large variability in the Martian atmospheric density, mapping along-track position becomes unacceptably uncertain after a few orbits. These methods essentially shift the time of periapsis of subsequent passes based on the measured drag during a pass. A similar method was tested and validated during Odyssey aerobraking [5]. This validated method was successfully implemented during the Mars Reconnaissance Orbiter aerobraking phase to shift the maneuver sequence.

During the Mars Odyssey mission, which used a much more aggressive strategy aerobraking than MRO, extensive thermal analyses were performed daily to predict the solar array temperature based on the freestream heat flux from prior orbits. These predictions were compared with measured temperatures to validate and tune the preflight thermal models and confirm maneuver boundaries. The weak link in the process was the model used for the Martian atmosphere. The model had to be calibrated using radio tracking data, and the heat flux predicted by the model had to be decreased by as much as 60% to be compatible with navigation results. Even so, the model could still not capture the actual shape of the density profile for many orbit passes (see Fig. 1) or the orbit-to-orbit variability, which varied between 10% inside the calm region within the northern latitudes to 40% at lower latitudes. This figure presents the atmospheric density recovered from the accelerometer data ("Accel") at a typical periapsis altitude (approximately 100 km) and the scaled model used by the project ("Mars-GRAM") [8]. Heat flux is proportional to density times the velocity cubed. Nevertheless, aerobraking operations continued to use maximum heat flux as the control variable.

An approach that used measured solar array temperatures as the control variable was proposed as a means of removing the dependence on surrogate variables [7]. This approach proposed using an empirically derived relationship between measured solar array temperature and maximum heat flux during operations. A predictive filter was proposed to make the decision on whether to perform orbital maneuvers to either raise or lower periapsis based only on the filtered heat flux. In addition, work began on using response surfaces to relate heat flux to maximum temperature, and this approach was used successfully during MRO [9]. The purpose of this paper is to integrate the thermal response surface methodology with previous autonomous aerobraking algorithms to completely eliminate the dependence on surrogate variables.

II. Mars Aerobraking Design

The three Mars aerobraking missions to date have flown the aerobraking phase with an upper and lower boundary or "corridor" on dynamic pressure or heat rate on the solar panels. Mars Global Surveyor was required to use dynamic pressure as the corridor upper limit because of the damage to the solar panel during the cruise phase. The dynamic pressure on the panel was limited to ensure no further damage during the aerobraking phase [10]. Both Mars Odyssey in 2001 and Mars Reconnaissance Orbiter (Fig. 2) in 2006 used a heat rate corridor upper limit. This heat rate limit was used as the surrogate variable for making maneuver decisions to determine whether to increase atmospheric density, and hence maximum heat rate, by lowering periapsis altitude or conversely raising periapsis altitude and reducing heat rate. Heat rate was used because it could be derived from onboard accelerometer measurements or estimated from the orbit-determination process. Further, maximum heat rate is a convenient variable for mission simulations because there was no direct method to correlate temperature predictions to predictive simulation techniques. Before aerobraking operations, the temperature limit of the solar panels was correlated to a heat rate limit for use by the flight mechanics simulations. On all three missions, the lower corridor limit was set by the mission requirement to end aerobraking with an orbit having a specified local solar time at the ascending node of the orbit. This constraint essentially defined the day on which aerobraking had to end.

The flight qualification limit for the spacecraft solar panels was 195°C. The flight allowable thermal limit was set at 175°C for Mars Odyssey and MRO to provide a safety margin. The amount of margin necessary to ensure a safe aerobraking phase is debatable. In previous Mars aerobraking missions, the amount of thermal margin on the spacecraft depended on the amount of time necessary to complete aerobraking. Mars Odyssey was required to complete aerobraking at

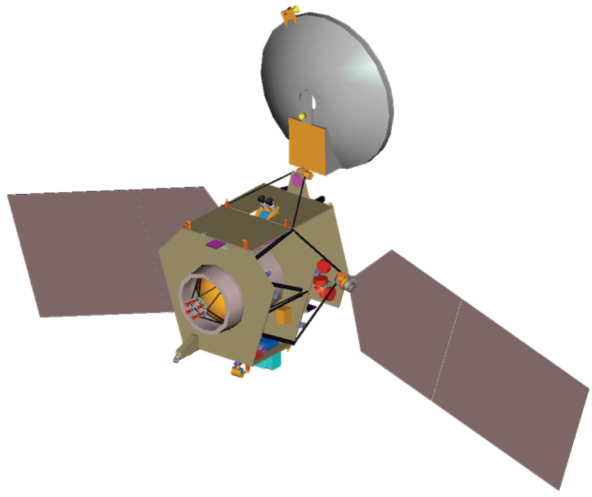

Fig. 2 MRO in aerobraking configuration.

a 3:00 p.m. local mean solar time (LMST). Because of the amount of time provided between Mars arrival and the beginning of the science phase, Odyssey was required to fly at higher heat rates, reducing the safety margin to 80–100%. This margin was calculated as the difference between the maximum heat rate for each orbit to the maximum allowable temperature on the spacecraft converted to a corresponding maximum heat rate. For the aerobraking phase of MRO, there were six months available for aerobraking between Mars orbit insertion and the necessary final LMST required for the science phase. Allotting six months for aerobraking allowed for more thermal margin on the spacecraft. In the design phase, the margin was an estimated 250%.

The conversion from the spacecraft maximum temperature limit to a maximum heat rate limit requires an assumed heating profile. The Mars density profiles were represented using a traditional isothermal atmosphere with a Gaussian uncertainty distribution. The upper heat rate limit for MRO was set such that the nominal profile would complete aerobraking at 3:00 p.m. LMST [11]. The lower boundary was set, as in previous missions, by the orbit geometry at the end of the aerobraking phase. Because of the LMST requirement, the thermal constraints on the spacecraft were not restricting and MRO could fly to lower temperatures than Odyssey. A typical temperature distribution from the thermal model of the MRO solar panel is shown in Fig. 3. The red portions of the solar panel image represent the warmest temperatures that the solar panel withstood for this drag pass (periapsis 55), and, in this instance, the maximum solar array temperature was estimated to be approximately 8°C. The maximum temperature that the MRO solar panels experienced during the entire mission was estimated to have been approximately 40°C. The maximum temperature during the Odyssey mission occurred on the anomalistic orbit 106 and was estimated at 135°C [12].

III. Autonomous Aerobraking with Heat Rate Constraint

For autonomous aerobraking, a simulation has been designed to predict ahead a few orbits to determine what effects the Mars gravity perturbations and drag will have on subsequent orbits and whether or not a maneuver is needed. Solar pressure and gravity perturbations may also be required in the actual implementation onboard the spacecraft. Inclusion of such terms is straightforward and not considered any further here, nor are they simulated in the described autonomous aerobraking strategy. It is assumed that the onboard ephemeris will be occasionally updated by the orbit-determination team; however, no estimates are made herein of the required update frequency.

For fully autonomous aerobraking, the onboard measurements of acceleration during the drag pass will be used directly in the equations of motion. Consequently, no global atmospheric model will be necessary. However, to predict drag for subsequent orbits, a model is required for maneuver decision purposes. First, drag acceleration is defined in the usual manner:

$$a_y = \frac{\rho V^2 C_y A}{2m} \tag{1}$$

Atmospheric density ρ can be obtained from Eq. (1) by using accelerometer data a_y, relative velocity V, drag coefficient C_y (here assumed constant), area A, and mass m. Next, assuming a standard exponential model for density where ρ_0, h_0, and h_s are the density, altitude, and atmospheric scale height at any given reference altitude, and r and h are the local density and altitude,

$$\rho_{\text{nom}} = \rho_0 \exp[-(h - h_0)/h_s] \tag{2}$$

The natural logarithm of Eq. (2) results in a linear equation in altitude h, and a least-squares fit is used to determine reference density ρ_0 and scale height h_s at a particular reference altitude h_0 (in most cases, this reference altitude is the periapsis altitude). These two parameters, ρ_0 and h_0, are then used to predict density for subsequent orbits using Eq. (3). In addition, a sliding least-square fit using these density and scale height values would be used to determine any wave structure in the atmosphere [13]. In the simulations, a simple atmospheric model with linear scale heights over specified altitude ranges is used along with the wave model and statistics from [13]. These statistics account for all of the processes discussed previously. Hence, in the simulations, density is modeled as

$$\rho(h, \phi, \lambda) = \rho_{\text{nom}}(h, \phi)\left[A_0 + S(t) + \sum_{n=1}^{3} A_n \sin n(\lambda - \lambda_n)\right] \tag{3}$$

where ρ_{nom} is the density at any given reference altitude as a function of that reference altitude and latitude from the linear scale height model. A_n is the amplitude as a fraction of ρ_{nom}, λ is east longitude, and λ_n is the phase of wave number n stationary-longitudinal wave. A_0 is a random variable with mean 1 and standard deviation between 0.15 and 0.19 [13]. The randomness in A_0 accounts for unmodeled variations in the atmosphere and errors due to the density and scale height estimation process. S is included to simulate a dust storm. During MGS, a regional dust storm caused density to increase by more than a factor of 2 in a few orbits. Any onboard autonomous algorithm will have to account for such storms either by modeling the dust storm and inflating the altitude at which the sensible atmosphere is detected, or accounting for the possibility of storms with extra margin. The remaining term represents three stationary waves. Amplitude and phases are given in [13] and, except for the storm term, the model is the same as that given in [13].

A simulated example of autonomous aerobraking, using a similar heat rate corridor to what was designed for MRO aerobraking, is shown in Fig. 4. The + symbols indicate where an apoapsis propulsive maneuver (ABM) has occurred. This simulated mission is similar to actual flight operations. During MRO aerobraking operations, 26 maneuvers occurred in the 145 days of aerobraking, maintaining approximately 150–250% margin. This simulation produces 17 maneuvers in 145 days of aerobraking. Note that maneuvers in the autonomous aerobraking simulation are performed solely on the basis of the heating corridor. Lifetime constraint and collision avoidance issues are not taken into account here but will be necessary in actual flight autonomy.

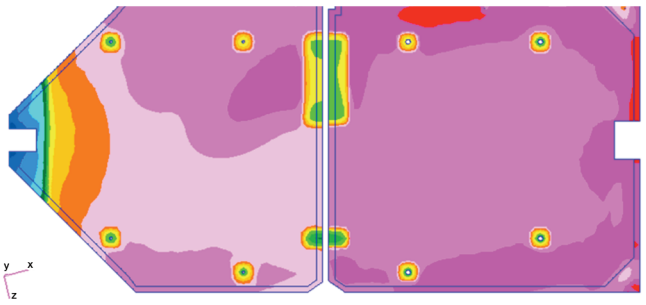

Fig. 3 MRO solar array temperatures for periapsis 55.

IV. Thermal Response Surface Analysis

A. Thermal Response Surface Model

A response surface is a simplified empirical model generally based on a more complex numerical model, in this case, a high-fidelity finite element thermal model. In this implementation, the response surface is a quadratic equation which is derived from the finite element model [9]. Using the design of experiments technique [9], the finite element model is systematically run, whereby each run is performed using a different set of analysis input parameters. The analysis input parameters used are those assumed to be the most significant or most influential in the analysis. In the case of the thermal analysis of the solar panels, variables fall into three categories: 1) environmental, such as the maximum atmospheric density, orbital period, and spacecraft velocity, 2) material property, such as M55J graphite composite face sheet emissivity, and 3) modeling variables, such as mass distribution. Using standard regression techniques, the coefficients of the response surface

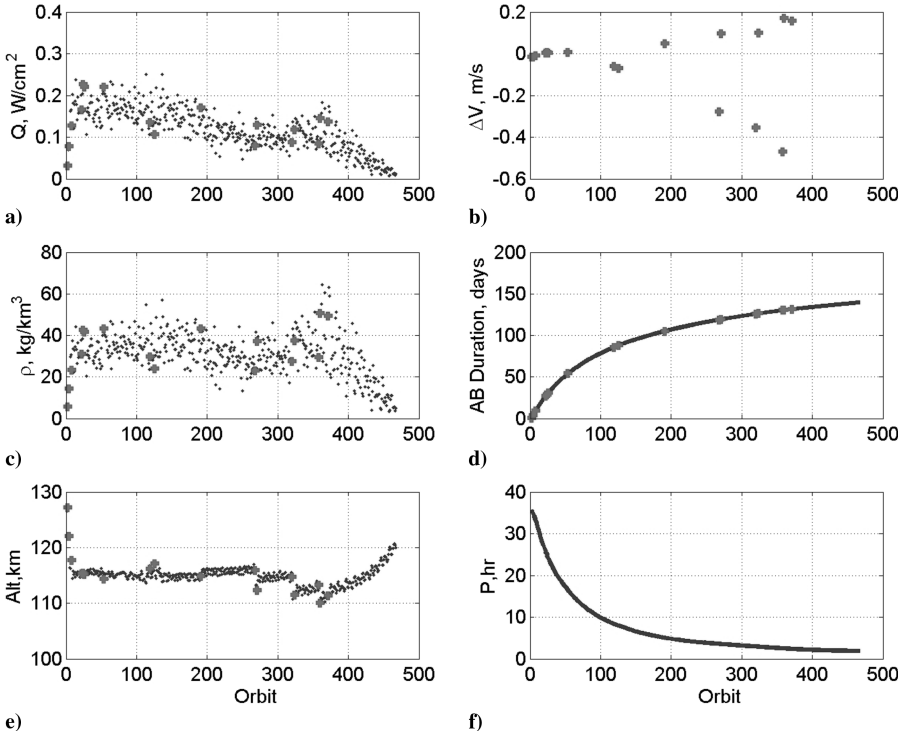

Fig. 4 Simulation results from a heat-constraint autonomous aerobraking strategy: a) periapsis heat rate, b) aerobraking maneuver magnitude, c) periapsis density, d) aerobraking duration, e) periapsis altitude, and f) spacecraft orbital period.

equation are determined, where the regression data are the temperature results from the finite element thermal model runs. The response surface equation is then just simply a quadratic equation for the peak solar panel temperature that is a function of the significant analysis parameters. For an operational aerobraking spacecraft, the only parameters that would vary orbit-to-orbit would be the environmental inputs. The response surface equation, however, is only valid for a single discrete point on the solar panel. To track different locations, like the locations of the thermal sensors on the solar panel, multiple response surface equations are required. The advantage is clear: the response surface is a simple equation that can be evaluated in seconds, as opposed to the finite element thermal model which takes an hour or more to run. Therefore, when given inputs such as maximum density, orbital period, and spacecraft velocity, it can be used to evaluate the temperatures of the solar panels of a given drag pass, in real time onboard the spacecraft. The calculation speed also allows a Monte Carlo simulation to be performed in real time. With the Monte Carlo simulation results, for a given orbit, a 3-σ temperature bound can be estimated and the probability of reaching the solar panel temperature limit can be calculated.

Thermal response surface analysis was first used for a spacecraft orbiting Mars during the Mars Reconnaissance Orbiter mission [9]. The analysis was validated during the aerobraking operations phase of the MRO mission and this analysis was later verified against the 2001 Mars Odyssey aerobraking phase. An example of the MRO thermal analysis using response surface is shown in Fig. 5. This figure shows that, given a very short calibration period of just a

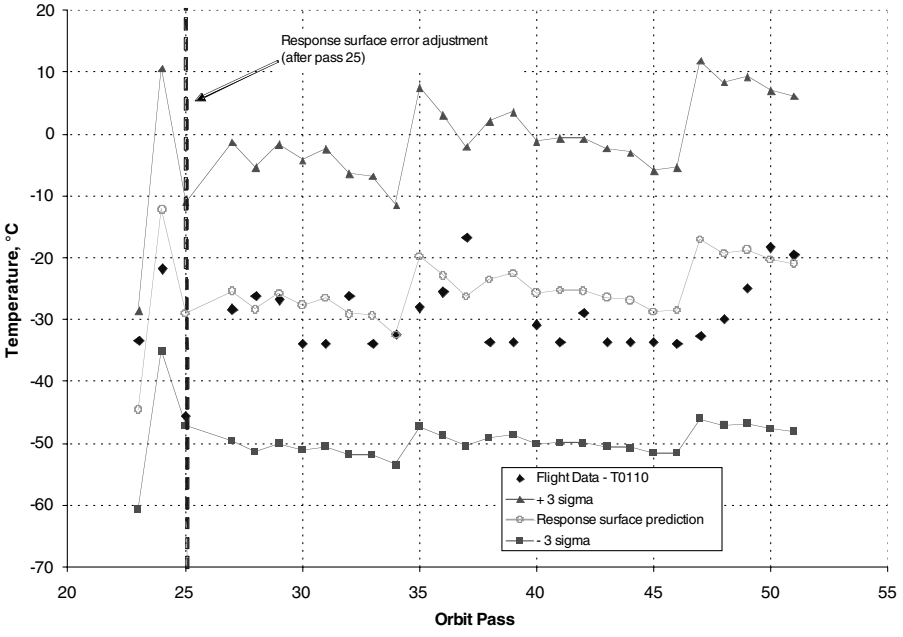

Fig. 5 Comparison of response surface temperature predictions with flight data.

couple of orbits, the response surface can predict the temperature of the solar panel very accurately. For the 27 orbits shown, all flight data from the spacecraft were within 15 deg of the response surface prediction and were well within the 3-σ prediction of the temperature on the solar arrays. Figure 5 is an example of a prediction of the thermocouple T0110. Several discrete thermocouples were placed on the solar panel, covering various temperature regimes on the front and back sides of the panel. All thermocouples, as well as the maximum predicted temperature of the entire solar panel (not necessarily at a thermocouple location), were modeled and predicted throughout the duration of the aerobraking phase.

Prediction of the solar panel temperatures is a key element required for autonomous aerobraking. In earlier studies [6], it was shown that, with a low-order gravity field, numerical integrator, and an adaptive atmospheric density model, the spacecraft can autonomously predict ahead a few orbits. Including the thermal response surface analysis allows autonomous direct prediction of the temperature of the spacecraft to within a few degrees. In addition, the response surface permits prediction of the uncertainty in the temperature. The spacecraft can then use a temperature corridor, rather than the dynamic pressure or heat flux corridor of previous missions. A temperature corridor more directly limits the vehicle based on the actual vehicle constraint: the temperature of the most limiting component, which for all the previous aerobraking missions was the solar panels.

The thermal response surface analysis was performed during aerobraking flight operations, but was not incorporated into trajectory simulations. Trajectory data were output to the thermal team at NASA Langley and then integrated into the thermal model [14]. The thermal response analysis was used to estimate the maximum temperature of the solar panels and determine how close to the thermal limit that the estimated 3-σ high temperature would be. Analysis of mission statistics was performed on a weekly basis. An example of the operational use of the thermal response surface is shown in Fig. 6.

The data lines beneath the error bars on this prediction represent the maximum predicted temperature on the MRO solar array. The black error bars show the 3-σ high error estimate from the response surface analysis. This particular analysis started from periapsis 52 and indicated that the maximum plus 3-σ temperature was less than 75°C, which resulted in more than 150% thermal margin on the spacecraft. The thermal limit line of the solar panel is constant at 175°C, as shown by the solid line at the top of the figure.

B. Autonomous Aerobraking Simulation Using Thermal Response Surface Algorithm

The previously described autonomous aerobraking simulation was enhanced by the addition of the thermal response surface algorithm. The analysis that was used to model the temperature of the solar panels during the MRO aerobraking phase was incorporated into the autonomous prediction capability of the simulation. Using the atmospheric density prediction described previously, a calculation for the drag duration, and the predicted period of the spacecraft, the maximum temperature of the solar panels is predicted for the subsequent three drag passes. The mean temperature prediction is used to evaluate the current and future position with respect to the defined temperature corridor. If outside the corridor, a single deterministic thermal response run is used to determine the desired density that would place the spacecraft to the desired temperature. A maneuver is performed at apoapsis based on the desired density and the predicted density. This maneuver logic is used throughout the simulated aerobraking phase and maintains temperatures similar to those seen during the MRO aerobraking phase. The results of this maneuver strategy using the thermal response surface algorithm are shown in Figs. 7 and 8. It is shown that this maneuver strategy maintains similar heat rates and densities of MRO, plotted in Figs. 7a and 7c, with approximately as many aerobraking orbits, reducing the orbital period from 36 h to less than 2 h, shown in Fig. 7f.

The spacecraft solar panel temperatures shown in Fig. 3 illustrate the large amount of margin on the solar panels that was exercised during MRO aerobraking operations (approximately 150–250%). This large margin was desired to reduce risk during the aerobraking phase because the science orbit required a 3:00 p.m. LMST. If this requirement were not applied to the MRO mission, the aerobraking phase may have been reduced and the margin would have been smaller. It can be seen in Fig. 8 that the maximum temperatures of the solar array do not exceed approximately 50°C, and the 3-σ high estimates of predicted temperature do not exceed approximately 85°C, well below the flight allowable limit of 175°C. As in Fig. 4, the + symbols indicate where an ABM has occurred to raise or lower periapsis altitude.

To emphasize the reduction in aerobraking duration that flying a reduced margin would allow, the autonomous aerobraking simulation was performed such that the margin was reduced. Results are illustrated in Fig. 9 and show that the duration of the aerobraking phase, while maintaining 200% margin (from the

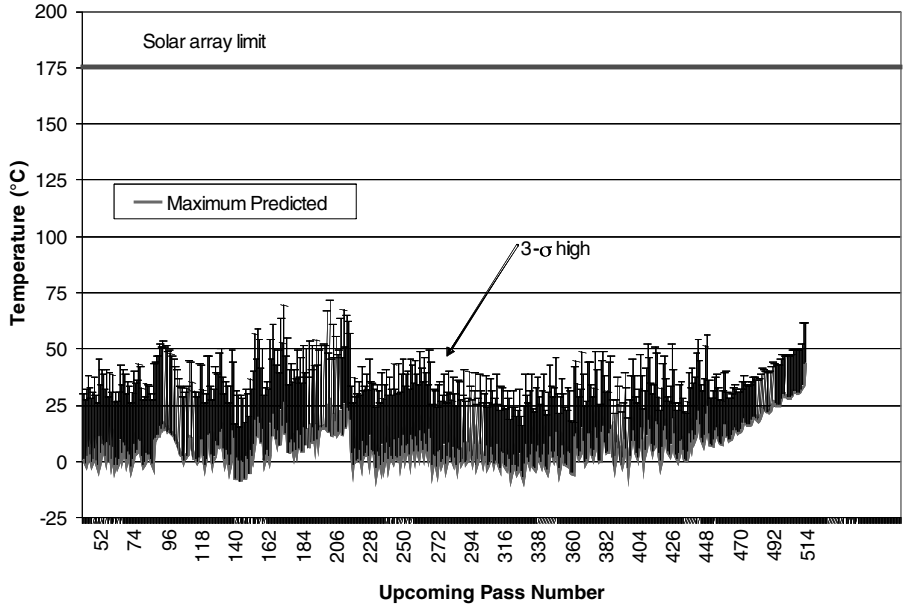

Fig. 6 Predicted MRO solar array maximum temperatures from response surface analysis.

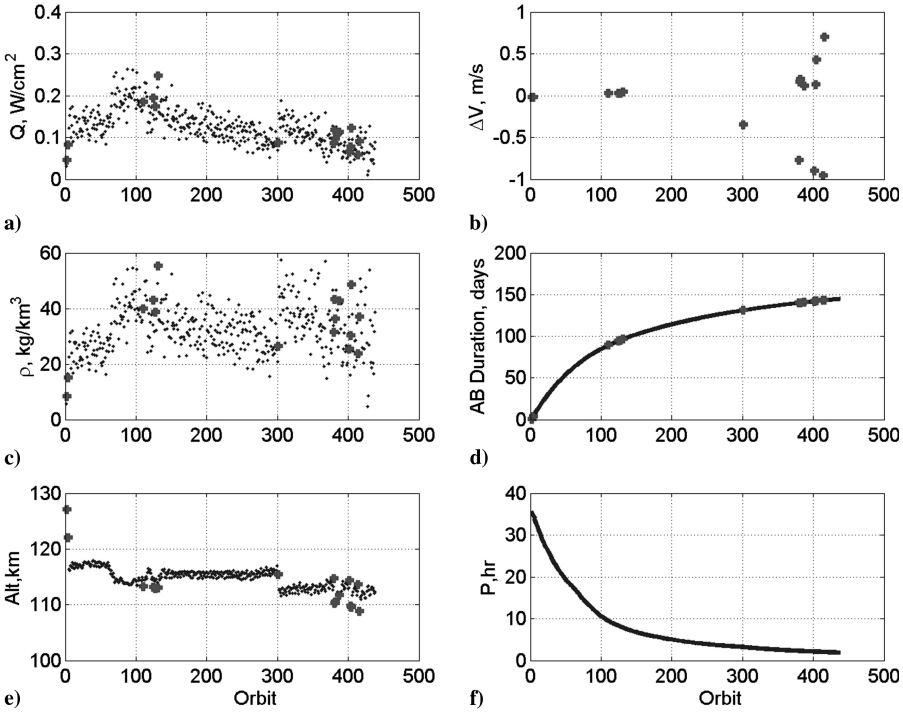

Fig. 7 Simulation results from a thermal response surface autonomous aerobraking strategy: a) periapsis heat rate, b) aerobraking maneuver magnitude, c) periapsis density, d) aerobraking duration, e) periapsis altitude, and f) spacecraft orbital period.

nominal predicted temperature), is 100 days. Likewise, aerobraking duration is 89 days for 150% margin and 73 days for 100% margin. Even in the 100% margin case, the 3-σ high temperature on the solar panel does not exceed the flight allowable limit of 175°C. Again, lifetime constraint and collision avoidance maneuvers are not taken into consideration in this simulation. Actual durations may be slightly longer due to the reduction of heating necessary toward the end of aerobraking to avoid violation of the lifetime constraint.

V. Conclusions

Aerobraking has been used in four previous missions to reduce the orbital period and eccentricity of spacecraft. Based on this heritage, it will likely be used for future planetary orbiting spacecraft as well. Aerobraking, however, can take many months and can require a large operational staff to support it. Developing a method of autonomy is necessary to reduce operational risk and cost. It has been shown that, in addition to using onboard measurements of acceleration during the drag pass and propagation of the spacecraft over time, a thermal response surface algorithm can be used to consistently predict the maximum temperature of the spacecraft with estimated uncertainties. This thermal response surface algorithm was developed and compared with MRO spacecraft telemetry, and used in a predictive sense in the autonomous aerobraking simulation. This capability of identifying the subsequent maximum temperatures on the spacecraft allows the spacecraft to maneuver to a higher or lower temperature

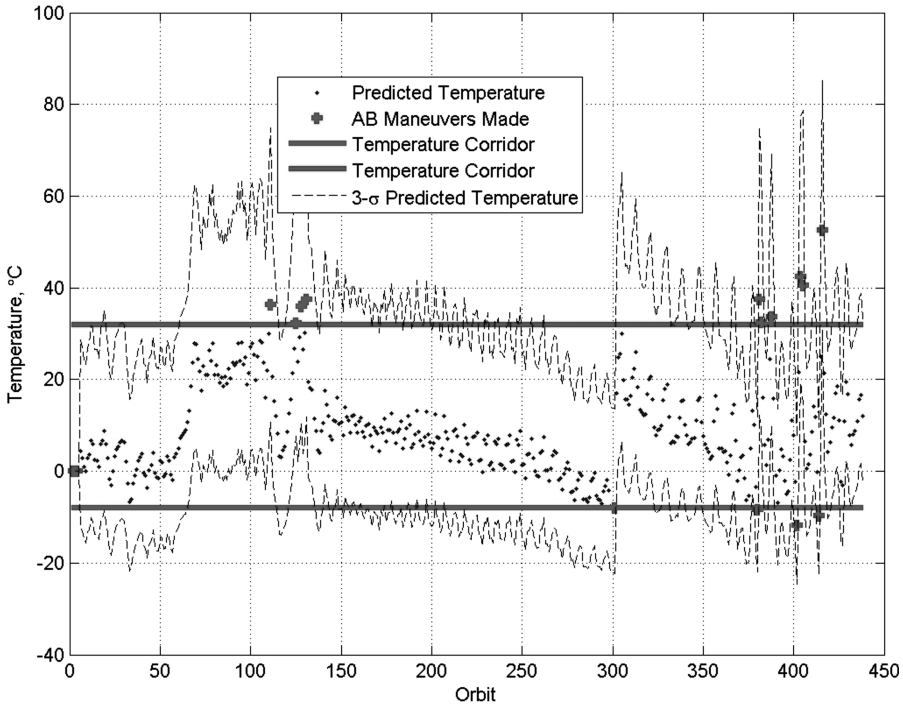

Fig. 8 Temperature profile of autonomous aerobraking simulation using thermal response surface analysis.

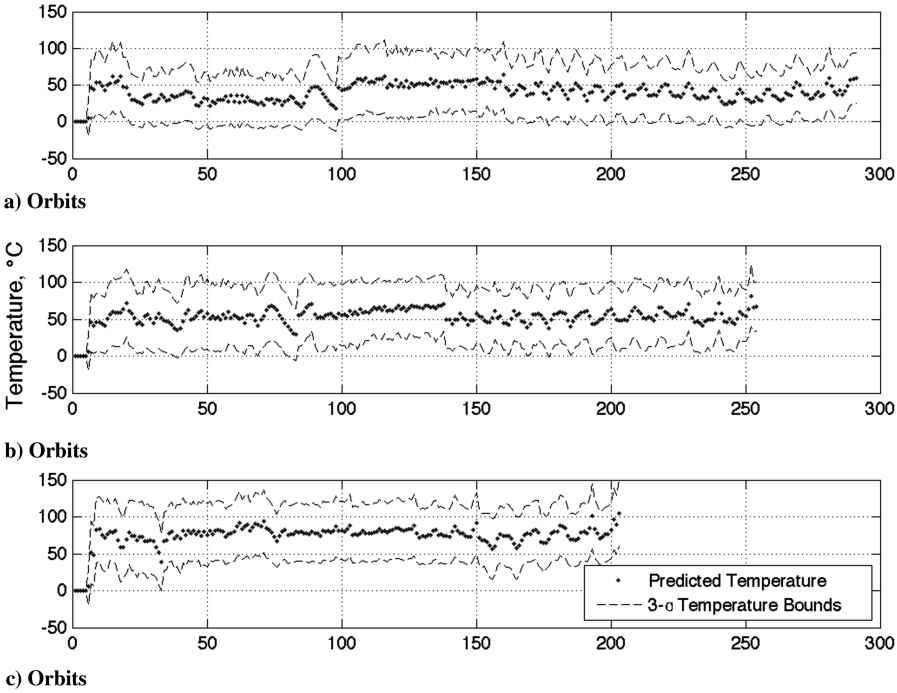

Fig. 9 Effect of reduced thermal margin on aerobraking duration: a) 200% margin, b) 150% margin, c) 100% margin.

region on subsequent orbits to avoid overheating the spacecraft, while aerobraking effectively within a desired time frame. This quick and effective tool is convenient and valuable in facilitating methods for autonomy in aerobraking operations.

References

[1] Lyons, D., Beerer, J., Esposito, P., Johnston, M. D., and Willcockson, W., "Mars Global Surveyor: Aerobraking Mission Overview," *Journal of Spacecraft and Rockets*, Vol. 36, No. 3, 1999, pp. 307–313. doi:10.2514/2.3472

[2] Smith, J., and Bell, J., "2001 Mars Odyssey Aerobraking," *Journal of Spacecraft and Rockets*, Vol. 42, No. 3, 2005, pp. 406–415. doi:10.2514/1.15213

[3] Lyons, D., "Mars Reconnaissance Orbiter: Aerobraking Reference Trajectory," AIAA Paper 2002-4821, Aug. 2002.

[4] Tolson, R. H., Bemis, E., Zaleski, K., Keating, G., Shidner, J., Brown, S., Brickler, A., Scher, M., Thomas, P., and Hough, S., "Atmospheric Modeling Using Accelerometer Data During Mars Reconnaissance Orbiter Aerobraking Operations," American Astronautical Society/AIAA Paper 07-183, Jan. 2007.

[5] Willcockson, W., and Johnson, M., "Mars Odyssey Aerobraking: The First Step Towards Autonomous Aerobraking Operations," IEEE Paper 1169, March 2003.

[6] Hanna, J. L., and Tolson, R. H., "Approaches to Autonomous Aerobraking at Mars," *Journal of the Astronautical Sciences*, Vol. 50, No. 2, April–June 2002, pp. 1257–1271.

[7] Hanna, J. L., Tolson, R. H., Cianciolo, A. M. D., and Dec, J. A., "Autonomous Aerobraking at Mars," *5th International ESA Conference on Guidance Navigation and Control Systems and Actuator and Sensor Product Exhibition, 2002*, ESA Paper SP-516, Feb. 2003.

[8] Tolson, R. H., Keating, G. M., George, B. E., Escalera, P. E., Wermer, M. R., Dwyer, A. M., and Hanna, J. L., "Application of Accelerometer Data to Mars Odyssey Aerobraking and Atmospheric Modeling," *Journal of Spacecraft and Rockets*, Vol. 42, No. 3, May–June 2005, pp. 435–443. doi:10.2514/1.15173

[9] Dec, J. A., "Probabilistic Thermal Analysis During Mars Reconnaissance Orbiter Aerobraking," AIAA Paper 2007-1214, Jan. 2007.

[10] Tolson, R. H., Keating, G. M., Cancro, G. J., Parker, J. S., Noll, S. N., and Wilkerson, B. L., "Application of Accelerometer Data to Mars Global Surveyor Aerobraking Operations," *Journal of Spacecraft and Rockets*, Vol. 36, No. 3, May–June 1999, pp. 323–329. doi:10.2514/2.3474

[11] Johnston, M. D., Graf, J. E., Zurek, R. W., Eisen, H. J., and Jai, B., "The Mars Reconnaissance Orbiter Mission," *Inst. of Electrical and Electronic Engineers Aerospace Conference*, Inst. of Electrical and Electronic Engineers Paper 1174, March 2004.

[12] Dec, J., and Gasbarre, J., "Thermal Analysis and Correlation of the Mars Odyssey Spacecraft's Solar Array During Aerobraking Operations," AIAA Paper 2002-4936, Aug. 2002.

[13] Dwyer, A. M., Tolson, R. H., Munk, M. M., and Tartabini, P. V., "Development of a Monte Carlo MarsGRAM Model for Mars 2001 Aerobraking Simulations," *Journal of the Astronautical Sciences*, Vol. 50, No. 2, April–June 2002, pp. 1293–1308.

[14] Prince, J. L. H., and Striepe, S. A., "NASA Langley Simulation Capabilities for the Mars Reconnaissance Orbiter," American Astronautical Society/AIAA Paper 2005-217, Jan. 2005.

C. Kluever
Associate Editor